analytical chemistry

pubs.acs.org/ac Article

Double Hairpin DNAs Recognition Induced a Novel Cascade Amplification for Highly Specific and Ultrasensitive Electrochemiluminescence Detection of DNA

Xiaoli Zhang, Ying Zhou, Yaqin Chai,* and Ruo Yuan*

Cite This: *Anal. Chem.* 2021, 93, 7987−7992 Read Online

ACCESS | Metrics & More | Article Recommendations | Supporting Information

ABSTRACT: Herein, a novel DNA cascade amplification, including double hairpin DNAs recognition-triggered single-target recycling (D-STR) and concatenated DNA structure-controlled rolling circle amplification (C-RCA), was developed as a signal amplifier to construct a highly specific and ultrasensitive electrochemiluminescence (ECL) biosensor for human immunodeficiency virus (HIV) DNA fragments detection, which not only revealed tremendous potential in avoiding false positive signals but also obviously promoted the amplification efficiency simultaneously compared to conventional single recognition of the target. Once the target DNA triggered the rolling circle amplification (RCA), the obtained RCA products could be anchored on the Pt-modified glassy carbon electrode (GCE) *via* the Pt−N bond, capturing massive ruthenium (Ru)-labeled ssDNA as the ECL signal tag to generate remarkable ECL emission. As a result, the proposed biosensor showed highly specific and ultrasensitive detection of the target with the detection limit down to 27.0 aM, which gives great impetus to the development of a novel specific biosensor for practical bioanalysis and diagnostic technologies.

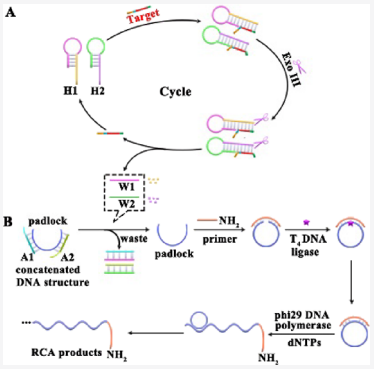

INTRODUCTION

Detection of specific DNA sequences and discrimination of single-nucleotide polymorphisms (SNPs) are significant for predicting disease predisposition and drug effectiveness.[1,2] Thus, it is of critical importance to enhance the specificity of nucleic acid detection. Recently, many nucleic acid amplification strategies, such as hybridization chain reaction (HCR),[3] catalytic hairpin assembly (CHA),[4] polymerase chain reaction (PCR),[5] strand displacement amplification (SDA),[6] and rolling circle amplification (RCA),[7] have widely emerged in biosensing, clinical diagnosis, and treatments.[8−10] Usually, single-recognition strategies based on the abovementioned traditional amplification technologies were developed owing to sequence specificity, but one or two nucleotide substitution in the target could not been distinguished from a perfectly matched target, which would lead to distinct false positive signals to interfere the accurate detection. Although some efforts have been dedicated for promoting the specificity of nucleic acid recognition, for instance, the introduction of locked nucleic acid (LNA) with high discrimination capability or nanomaterials with strong interaction with biomarkers to construct a nucleic acid detection platform for enhancing the selectivity,[11−13] these approaches still encountered the disadvantage of complex operation and complicated procedures. Therefore, developing a convenient and highly specific method for nucleic acid sequence recognition is of utmost significance for practical biological applications. In this study, a double hairpin DNAs recognition-triggered single-target recycling (D-STR) was first proposed, in which two recognition parts were designed to severally discriminate nucleotide substitution of the target, so that it possessed the mutual correction function for remarkably improving the specificity of target recognition in comparison with single recognition of the target.

As a proof of concept, the D-STR and concatenated DNA structure-controlled rolling circle amplification (C-RCA) were employed to construct the electrochemiluminescence (ECL) sensing interface for the specific and ultrasensitive detection of human immunodeficiency virus (HIV) DNA fragments. By this way, the designed cascade amplification including D-STR and C-RCA also realized a significant progress in signal amplification efficiency. The corresponding principle and fabrication process of the proposed biosensor are exhibited in Scheme 1. Initially, two hairpin DNAs (H1 and H2) were introduced to synchronously discern different parts of the target for releasing two output DNAs (W1 and W2) with the aid of exonuclease III (Exo III). Subsequently, only in the simultaneous presence of two output DNAs, the concatenated DNA structure could be opened for releasing the padlock

Received: March 8, 2021
Accepted: May 12, 2021
Published: May 24, 2021

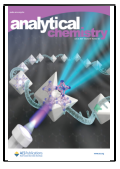

https://doi.org/10.1021/acs.analchem.1c01012
Anal. Chem. 2021, 93, 7987−7992

Scheme 1[a]

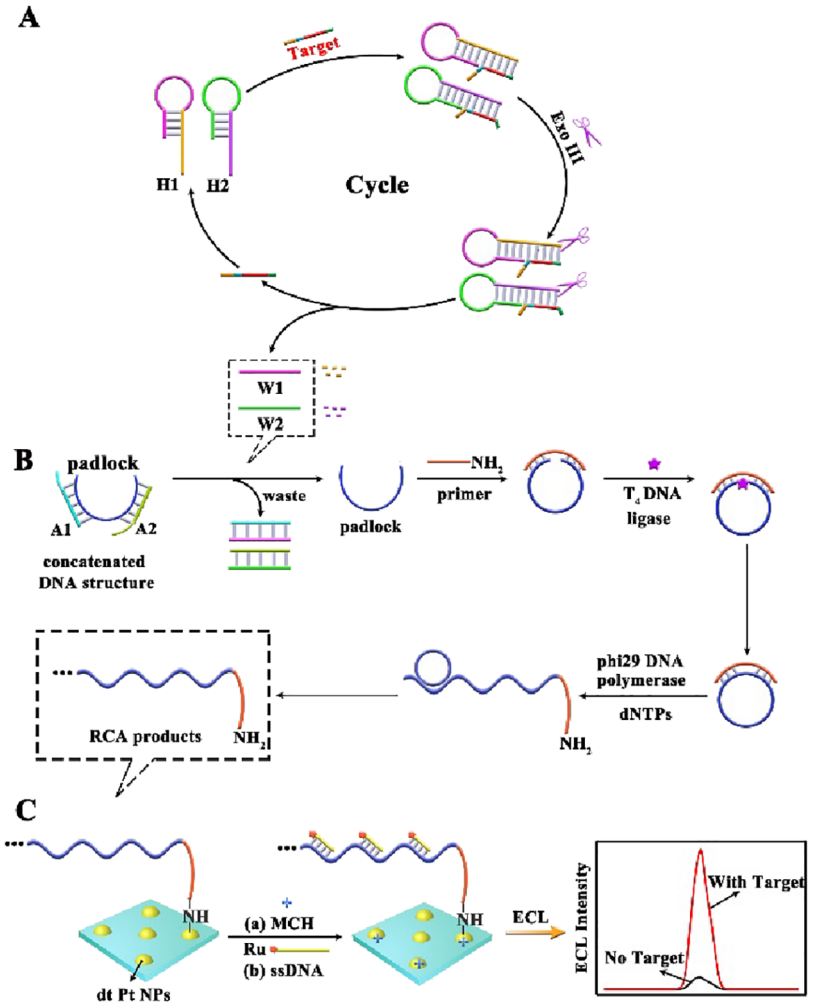

[a]Schematic description of the specific and sensitive biosensor for HIV DNA fragments detection based on (A) double-recognition-triggered single-target recycling and (B) concatenated DNA structure-controlled rolling circle amplification. (C) Construction process of the proposed ECL biosensor.

strands to initiate subsequent RCA reaction. Afterward, the obtained RCA products with amounts of repetitive DNA sequences could be anchored on Pt NPs-modified GCE through the Pt−N bond.[14,15] Then, plentiful ECL luminophore ruthenium (Ru)-labeled ssDNA strands were captured by the immobilized RCA products to generate strong ECL emission with tripropylamine (TPrA) as the coreactant for the ultrasensitive detection of HIV DNA fragments. In consequence, the elaborated biosensor performed a good linearity ranging from 100 aM to 100 pM with a low detection limit of 27.0 aM. The work also strongly evidenced that the D-STR has the great discrimination ability of the single-base mismatched sequence from the target, providing a new insight for specific detection of nucleic acid to hold great promise in clinical application.

EXPERIMENTAL SECTION

Exo III-Assisted Target Cycling Reaction. The DNA strands H1 and H2 were annealed at 95 °C for 5 min, followed by gradually cooling down to room temperature over 2 h for forming a stable hairpin structure.[16,17] First, 1 μM H1 and H2 was added in a tube; then, varieties of different concentrations of HIV DNA fragments were introduced for 2 h at 37 °C, and the exonuclease III (0.5 U/μL) was added for 1 h at 37 °C; then, the abovementioned solution was kept at 65 °C for 10 min to stop the enzyme reaction.

RCA Reaction. Initially, 1 μM padlock and A1 and A2 strands were hybridized at 37 °C for 2 h after annealing at 95 °C for 5 min. The as-prepared Exo III-assisted target cycling outputs were injected in the abovementioned tube for 2 h at 37 °C. Subsequently, 1 μM primer was introduced for 2 h at 37 °C. Then, 10× T4 DNA ligation buffer and 5 U/μL T4 DNA ligase were introduced overnight at 16 °C. Afterward, 10× phi29 buffer, 0.2 U/μL phi29 DNA polymerase, and 500 μM dNTPs were introduced for 2 h at 30 °C. Finally, the abovementioned solution was heated to 65 °C for 15 min to inactivate the enzyme.

Fabrication of the Biosensor. First, the glassy carbon electrode (GCE) was polished with 0.3 and 0.05 μm of alumina powder and rinsed with deionized water for further use. Then, the prepared electrode was immersed into $H_2PtCl_6 \cdot 6H_2O$ (1%) solution and electrodeposited at −0.25 V for 30 s to attain the platinum nanoparticles (Pt NPs)-modified layer. Subsequently, 10 μL of RCA products was anchored on the electrode overnight at 4 °C *via* the Pt−N bond. After being rinsed with deionized water, 10 μL of 6-mercapto-1-hexanol

https://doi.org/10.1021/acs.analchem.1c01012
Anal. Chem. 2021, 93, 7987−7992

(MCH, 1 mM) was incubated for 40 min at room temperature for blocking nonspecific binding sites. Ultimately, 10 μL of Ru-modified ssDNA was dropped on the sensing interface for 2 h at ambient temperature to obtain ECL signals.

ECL Detection. The proposed biosensor was tested in 2 mL of phosphate-buffered saline (PBS, pH = 7.4) including 15 mM TPrA to obtain the ECL signals using an MPI-A ECL analyzer. Additionally, the scanning potential varied from 0 to 1.25 V with a scan rate of 200 mV/s, and the photomultiplier tube high voltage was set as 800 V. The ΔI was the decreased value ($\Delta I = I - I_0$, I_0 indicated the ECL signals of the blank), while I expressed the ECL signals with various concentrations of target HIV DNA fragments.

RESULTS AND DISCUSSION

Feasibility Analysis of Double Hairpin DNAs-Triggered Single-Target Recycling (D-STR). The native polyacrylamide gel electrophoresis (PAGE, 16%) was utilized for investigating the feasibility of D-STR. As seen in Figure 1,

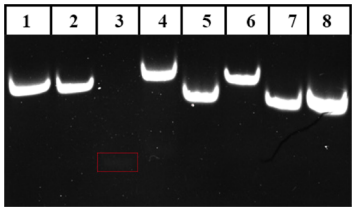

Figure 1. 16% native PAGE of the samples: lane 1, 1 μM H1; lane 2, 1 μM H2; lane 3, 1 μM HIV DNA (target); lane 4, 1 μM H1 + HIV DNA; lane 5, 1 μM H1 + HIV DNA with Exo III; lane 6, 1 μM H2 + HIV DNA; lane 7, 1 μM H2 + HIV DNA with Exo III; and lane 8, 1 μM H1 + H2 + HIV DNA with Exo III.

lane 1 (H1, 60 base) and lane 2 (H2, 60 base) were much higher than the lane 3 (HIV DNA fragments, 21 base), owing to the larger molecular weight. When HIV DNA fragments were introduced to recognize H1 (lane 4, H1 + T) or H2 (lane 6, H2 + T), respectively, it could be observed that lane 4 and lane 6 posed a higher position because H1 or H2 was successfully hybridized with HIV DNA fragments. After the addition of Exo III, a bright band was displayed in lane 5 (H1 + T with Exo III) and lane 7 (H2 + T with Exo III), confirming the successful generation of output DNA (W1 and W2). Furthermore, as shown in lane 8, when H1 and H2 were simultaneously added to recognize the target, a much thicker bright band with almost the same position as lane 6 and lane 7 was obtained in the presence of Exo III, indicating that the double hairpin DNAs recognition of HIV DNA fragments recycling was reasonable and practicable.

PAGE Analysis of Specificity. To further prove the specificity of the prepared biosensor, the PAGE (16%) was employed to characterize the discrimination ability from mismatched DNA sequences. As shown in Figure 2A, lane 3 was H1 + H2 + T, which was much lower than H1 (lane 1) and H2 (lane 2) because of the cleavage of Exo-III for H1 and H2 strands. Lane 4, lane 5, lane 6, and lane 7 corresponded to H1 + H2 + M1, H1 + H2 + M2, H1 + H2 + M2′, and H1 + H2 + M2″ in the presence of Exo III, respectively (M1 represented the single-base mismatched DNA and M2, M2′, and M2″ represented three different kinds of double-base mismatched DNA), and they all showed no distinct band of two outputs obtained in lane 3 because they could not be

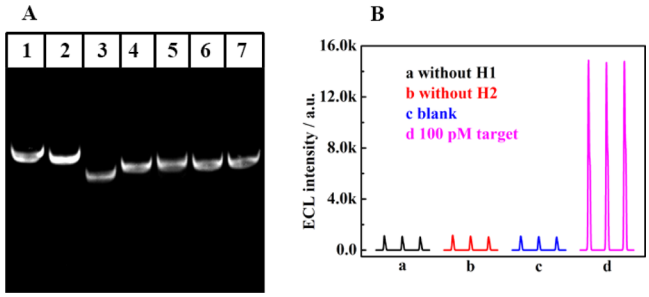

Figure 2. (A) 16% native PAGE analysis of different samples: lane 1, H1; lane 2, H2; lane 3, H1 + H2 + T with Exo III; lane 4, H1 + H2 + M1 with Exo III; lane 5, H1 + H2 + M2 with Exo III; lane 6, H1 + H2 + M2′ with Exo III; and lane 7, H1 + H2 + M2″ with Exo III. (B) ECL intensities of the proposed biosensor (a) in the absence of H1, (b) without H2, (c) in the absence of T, and (d) with 100 pM HIV DNA.

discerned to trigger the cleavage. The results exhibited discrimination ability of the single-base mismatched sequence, further proving the excellent specificity of the proposed biosensor.

Meanwhile, the single recognition of the target was characterized. In Figure 2B, curve a represented the ECL intensity in the absence of H1, while curve b showed the ECL response of the proposed biosensor without H2, and they all exhibited slight changes compared with the blank sample (curve c). However, the ECL intensity showed a great increase when 100 pM HIV DNA fragments were introduced (curve d). The results illustrated that only the H1 and H2 were simultaneously added to recognize the target, and the HIV DNA fragments could be detected. Thus, it could be concluded that compared with single recognition of the target, double hairpin DNAs recognition of the single target possessed a mutual correction function owing to the different discrimination abilities to different parts of the target, which extremely enhanced the specificity of target recognition.

CV and EIS Characterization of the Proposed Biosensor. To investigate the modification process of the ECL biosensing platform, cyclic voltammetry (CV) and electrochemical impedance spectroscopy (EIS) were characterized in 5 mM $[Fe(CN)_6]^{3-/4-}$ containing 0.1 M KCl. As shown in Figure 3A (CV), the bare GCE (curve a) showed a pair of obvious redox peaks. Moreover, after the deposition of Pt NPs, the current increased obviously due to high conductivity of Pt (curve b).[18] When RCA products (curve c) were immobilized on the electrode in succession, the redox peak current was decreased distinctly because the negatively charged DNA phosphate backbone would repulse $[Fe(CN)_6]^{3-/4-}$. Then, MCH (curve d) was dropped on the sensing interface for blocking nonspecific binding sites, and a declined redox current was observed owing to the impediment of MCH. Similarly, after incubation of ssDNA (curve e), the redox peak current was further decreased for the hindrance of ssDNA.

Simultaneously, as depicted in Figure 3B (EIS), compared with the bare GCE (curve a), the Pt-deposited GCE (curve b) showed a lower electron transfer resistance (R_{et}) owing to Pt facilitating electron transfer. When RCA products (curve c), MCH (curve d), and ssDNA (curve e) were modified on the electrode stepwisely, a series of increased R_{et} were obtained due to the obstruction of MCH and the nucleic acid.[19] These

https://doi.org/10.1021/acs.analchem.1c01012
Anal. Chem. 2021, 93, 7987−7992

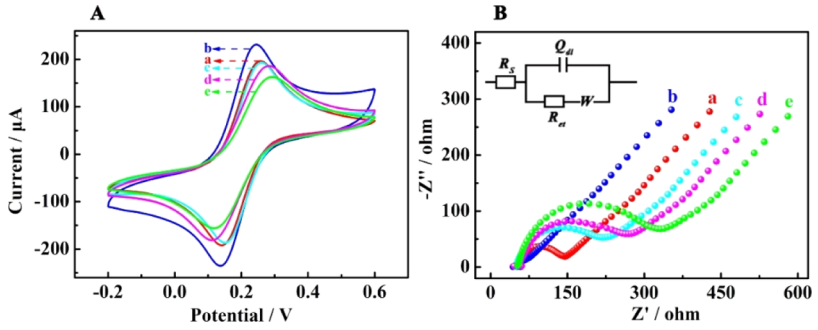

Figure 3. (A) CV curves of the (a) bare GCE, (b) Pt NPs/GCE, (c) RCA products/Pt NPs/GCE, (d) MCH/RCA products/Pt NPs/GCE, and (e) ssDNA/MCH/RCA products/Pt NPs/GCE in 0.1 M PBS (pH 7.4) containing 5.0 mM $[Fe(CN)_6]^{3-/4-}$ and 0.1 M KCl. (B) EIS diagram of the electrode assembly process (a) bare GCE, (b) Pt NPs/GCE, (c) RCA products/Pt NPs/GCE, (d) MCH/RCA products/Pt NPs/GCE, and (e) ssDNA/MCH/RCA products/Pt NPs/GCE in 0.1 M PBS (pH 7.4) containing 5.0 mM $[Fe(CN)_6]^{3-/4-}$ and 0.1 M KCl. Moreover, the inset showed the equivalent circuit diagram.

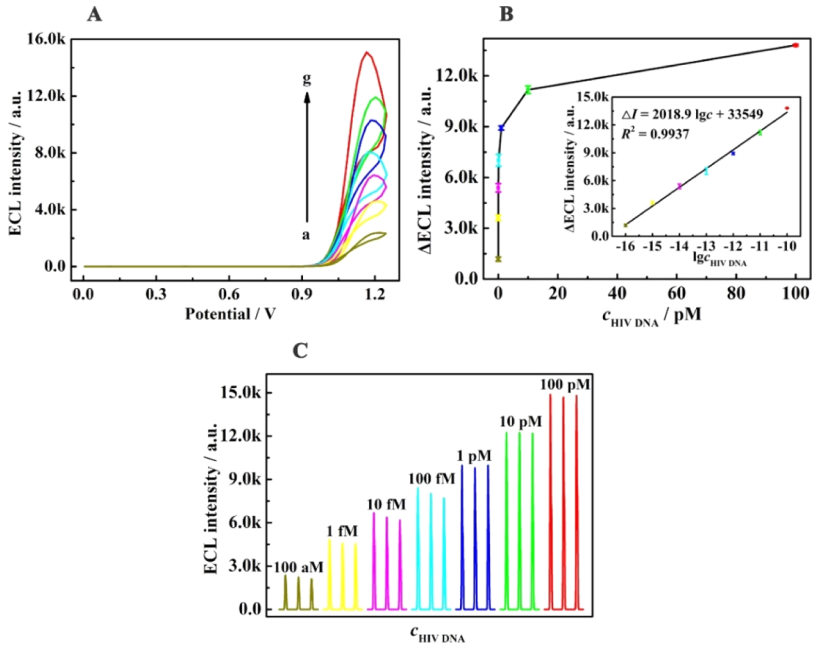

Figure 4. (A) ECL intensity−potential curves of the proposed biosensor incubated with HIV DNA fragments concentrations of 100 aM, 1 fM, 10 fM, 100 fM, 1 pM, 10 pM, and 100 pM (from a−g). (B) Relationship between ΔECL ($\Delta I = I_0 - I$) and the concentration of HIV DNA fragments. The inset: the calibration plot of ΔECL of the logarithm of HIV DNA fragments concentration. (C) Stability of different concentrations of HIV DNA fragments from 100 aM to 100 pM.

Table 1. Comparison of This Work with Other Methods

method	target	linear range	LOD	ref.
fluorescence	HIV DNA	0.025 nM to 500 nM	15 pM	20
fluorescence	HIV-1 RNAs	10 nM to 300 nM	2.06 nM	21
PEC[a]	HIV DNA	10 fM to 1 nM	1.16 fM	22
electrochemistry	HIV-1 gene	100 fM to 10 nM	150 fM	23
ECL	HIV DNA	0.05 pM to 50 nM	39.81 fM	24
ECL	HIV-1 gene	3 fM to 0.3 nM	0.3 fM	25
ECL	HIV DNA	100 aM to 100 pM	27.0 aM	this work

[a]Photoelectrochemical.

results were in good agreement with that observed in CV, further demonstrating the successful assembly of the biosensor.

ECL Responses of the Proposed Biosensor. To investigate the analytical performance of the developed biosensor, the ECL signals of various concentrations about HIV DNA were measured with the "off−on" mode under the optimum conditions (details are shown in Supporting Information, Figure S1). As demonstrated in Figure 4A, the ECL signals exhibited a monotonically increase with elevated concentrations of target HIV DNA fragments from 100 aM to 100 pM. While Figure 4B exhibited the relationship between ΔECL and the concentration of HIV DNA fragments, it was

https://doi.org/10.1021/acs.analchem.1c01012
Anal. Chem. 2021, 93, 7987−7992

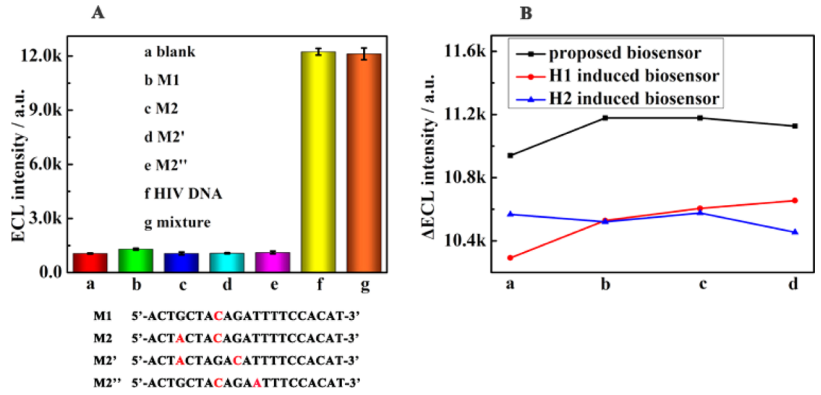

Figure 5. (A) Specificity of the proposed biosensor (a) blank, (b) 1 nM M1, (c) 1 nM M2, (d) 1 nM M2, (e) 1 nM M2″, (f) 10 pM HIV DNA fragments, and (g) mixture containing 10 pM HIV DNA, 1 nM M1, 1 nM M2, 1 nM M2′, and 1 nM M2″. (B) Difference value of ECL signals (the ECL intensity of HIV DNA subtract the ECL intensity of (a) M1, (b) M2, (c) M2′, and (d) M2″).

found that the developed biosensor manifested an excellent linear relationship between the ECL intensity and the logarithm of various concentrations of HIV DNA fragments (the inset of Figure 4B). The corresponding regression equation was ΔI = 2018.9 lg$c$ + 33,549 with a squared correlation coefficient of 0.9937. Moreover, the limit of detection (LOD) was down to 27.0 aM. The analytical performance of the proposed biosensor was contrasted with other detection strategies. As shown in Table 1, the fabricated biosensor exhibited a high sensitivity and a lower LOD, which demonstrated that it might have great application prospect in clinical bioassay.

Stability was a vital parameter for the performance of the developed biosensor. As observed in Figure 4C, the ECL signals of various concentrations about target HIV DNA fragments were relatively stable with three continuous scans, reflecting that the proposed biosensor exhibited fabulous stability.

Selectivity of the Proposed Biosensor. To further study the selectivity and specificity of the designed biosensor, the effect of single-base mismatched DNA (Sm-DNA) and three kinds of double-base mismatched DNA (Dm-DNA) about the ECL signals were monitored. To further monitor the specificity of the proposed biosensor, the concentrations of interfering substances (the mismatched DNA) were selected as 1 nM which were 100 times higher than that of 10 pM target HIV DNA fragments. As illustrated in Figure 5A, the ECL intensity changes in Sm-DNA and Dm-DNA (from column b to e) were negligible compared with the blank sample in the absence of target HIV DNA fragments (column a). Inversely, once a small amount of HIV DNA fragments (10 pM) were mixed with these interfering mismatched DNAs (column g), the ECL intensities were rapidly increased, which was almost same as the value obtained from 10 pM HIV DNA fragments (column f), indicating the high selectivity and specificity of the proposed biosensor.

Simultaneously, single recognition of the single target including the H1-induced biosensor (padlock strands were only locked by A1 strands) and H2-induced biosensor (padlock strands were only locked by A2 strands) was constructed for contrasting with the mismatch-base discriminability of the proposed biosensor (the selectivity of the H1-induced biosensor and H2-induced biosensor is shown in the Supporting Information). Thus, from Figure 5B, it represented the difference value of ECL intensity [the ECL signals of HIV DNA fragments subtract the ECL intensity of (a) M1, (b) M2, (c) M2′, (d) M2″] of different biosensors, and the difference value of ECL intensity of the proposed biosensor (black line) was distinctly higher than those of the H1-induced biosensor (red line) and H2-induced biosensor (blue line), manifesting the superior selectivity of the proposed biosensor, which further declared the ascendant specificity of D-STR.

Detection of HIV DNA Fragments in Clinical Serum Samples. The reliability of the proposed biosensor for HIV DNA fragments detection was evaluated by investigating the HIV DNA fragments in the human serum sample, which was acquired from Xinqiao Hospital (Chongqing, China). The experiment was carried out by the standard addition method through adding various concentrations of standard HIV DNA fragments into the 10-fold human serum diluted with 0.1 M PBS (pH = 7.4) buffer. As shown in Table 2, the recoveries of HIV DNA fragments varied from 96.32 to 110.4% with the relative standard deviation (RSD) of 1.59−4.51% for the HIV DNA fragments (n = 3), which manifested that the designed ECL sensing platform revealed the potential to be utilized in actual biological sample detection.

Table 2. Recovery Study Carried out in Serum Samples for HIV DNA Fragments Determination by the Proposed Biosensor (n = 3)

sample	spiked concentration/pM	found concentration/pM	recovery/%	RSD/%
1	50	50.12	101.7	3.04
2	10	11.04	110.4	3.69
3	1	1.040	104.0	1.95
4	0.1	0.09921	99.21	2.44
5	0.05	0.04816	96.32	2.94

CONCLUSIONS

In conclusion, to improve the specificity and sensitivity of the target detection, a novel cascade amplification based on D-STR and C-RCA was used to construct an ECL biosensor for HIV DNA fragments detection. First, unlike the single recognition of the target, the double-hairpin DNA recognition of the single target possessed a mutual correction function, so it had the inherent virtues to fabricate a single-step ECL biosensor with outstanding specificity for target HIV DNA fragments detection. Second, the concatenated DNA structure could be

https://doi.org/10.1021/acs.analchem.1c01012
Anal. Chem. 2021, 93, 7987−7992

opened only when two output DNAs were successfully acquired for the follow-up RCA reaction to detect the target, which further enhanced the specificity of this method. Significantly, the proposed strategy showed great potential as the new generation of specificity detection for biological applications.

■ ASSOCIATED CONTENT

Supporting Information

The Supporting Information is available free of charge at https://pubs.acs.org/doi/10.1021/acs.analchem.1c01012.

Materials and reagents, apparatus, native PAGE analysis process, cross-linking of ssDNA-NH_2 and Ru−COOH, optimization of experimental conditions, PAGE analysis of C-RCA, reproducibility of the proposed biosensor, selectivity of single recognition of the single target, and LOD calculation (PDF)

■ AUTHOR INFORMATION

Corresponding Authors

Yaqin Chai − *Key Laboratory of Luminescence Analysis and Molecular Sensing (Southwest University), Ministry of Education, College of Chemistry and Chemical Engineering, Southwest University, Chongqing 400715, PR China;* orcid.org/0000-0003-4392-9592; Phone: +86-23-68252277; Email: yqchai@swu.edu.cn; Fax: +86-23-68253172

Ruo Yuan − *Key Laboratory of Luminescence Analysis and Molecular Sensing (Southwest University), Ministry of Education, College of Chemistry and Chemical Engineering, Southwest University, Chongqing 400715, PR China;* orcid.org/0000-0003-3664-6236; Email: yuanruo@swu.edu.cn

Authors

Xiaoli Zhang − *Key Laboratory of Luminescence Analysis and Molecular Sensing (Southwest University), Ministry of Education, College of Chemistry and Chemical Engineering, Southwest University, Chongqing 400715, PR China*

Ying Zhou − *Key Laboratory of Luminescence Analysis and Molecular Sensing (Southwest University), Ministry of Education, College of Chemistry and Chemical Engineering, Southwest University, Chongqing 400715, PR China*

Complete contact information is available at: https://pubs.acs.org/10.1021/acs.analchem.1c01012

Notes

The authors declare no competing financial interest.

■ ACKNOWLEDGMENTS

This work was financially supported by the NNSF of China (21775124 and 21974108) and the Fundamental Research Funds for the Central Universities (XDJK2019TJ002), China.

■ REFERENCES

(1) Li, R.; Li, Y.; Fang, X.; Yang, H.; Wang, J.; Kristiansen, K.; Wang, J. *Genome Res.* **2009**, *19*, 1124−1132.

(2) Wolfe, M.; Ali, M.; Brennan, J. *Anal. Chem.* **2019**, *91*, 4735−4740.

(3) Zhu, L.; Ye, J.; Wang, S.; Yan, M.; Zhu, Q.; Huang, J.; Yang, X. *Chem. Commun.* **2019**, *55*, 11551−11554.

(4) Wei, Q.; Huang, J.; Li, J.; Wang, J.; Yang, X.; Liu, J.; Wang, K. *Chem. Sci.* **2018**, *9*, 7802−7808.

(5) Zou, L.; Ling, L. *Anal. Chem.* **2018**, *90*, 13373−13377.

(6) Huang, Z.; Luo, Z.; Chen, J.; Xu, Y.; Duan, Y. *ACS Sens.* **2018**, *3*, 2423−2431.

(7) Li, C.; Chen, H.; Hu, J.; Zhang, C. *Chem. Sci.* **2020**, *11*, 5724−5734.

(8) Deng, R.; Zhang, K.; Li, J. *Accounts Chem. Res.* **2017**, *50*, 1059−1068.

(9) Zhou, H.; Liu, J.; Xu, J.; Zhang, S.; Chen, H. *Chem. Soc. Rev.* **2018**, *47*, 1996−2019.

(10) Wang, Z.; Li, P.; Cui, L.; Qiu, J.; Jiang, B.; Zhang, C. *TrAC, Trends Anal. Chem.* **2020**, *129*, 115959.

(11) Zhang, Y.; Wang, L.; Luo, F.; Qiu, B.; Guo, L.; Weng, Z.; Lin, Z.; Chen, G. *Chem. Commun.* **2017**, *53*, 2910−2913.

(12) Xue, T.; Liang, W.; Li, Y.; Sun, Y.; Xiang, Y.; Zhang, Y.; Dai, Z.; Duo, Y.; Wu, L.; Qi, K.; Shiyananju, B.; Zhang, L.; Cui, X.; Zhang, H.; Bao, Q. *Nat. Commun.* **2019**, *10*, 28.

(13) Xu, G.; Abbott, J.; Qin, L.; Yeung, K.; Song, Y.; Yoon, H.; Kong, J.; Ham, D. *Nat. Commun.* **2014**, *5*, 4866.

(14) Liu, J.; Tang, Z.; Zhuo, Y.; Chai, Y.; Yuan, R. *Anal. Chem.* **2017**, *89*, 9108−9115.

(15) Legin, A.; Schintlmeister, A.; Jakupec, M.; Galanski, M.; Lichtscheidl, I.; Wagner, M.; Keppler, B. *Chem. Sci.* **2014**, *5*, 3135−3143.

(16) He, M.; Wang, K.; Wang, W.; Yu, Y.; Wang, J. *Anal. Chem.* **2017**, *89*, 9292−9298.

(17) Zang, Y.; Lei, J.; Ling, P.; Ju, H. *Anal. Chem.* **2015**, *87*, 5430−5436.

(18) Nie, Y.; Zhang, P.; Wang, H.; Zhuo, Y.; Chai, Y.; Yuan, R. *Anal. Chem.* **2017**, *89*, 12821−12827.

(19) Hua, X.; Yang, E.; Yang, W.; Yuan, R.; Xu, W. *Chem. Commun.* **2019**, *55*, 12463−12466.

(20) Chen, Y.; Duong, H.; Wen, S.; Mi, C.; Zhou, Y.; Shimoni, O.; Valenzuela, S.; Jin, D. *Anal. Chem.* **2018**, *90*, 663−668.

(21) Ma, Y.; Mao, G.; Huang, W.; Wu, G.; Yin, W.; Ji, X.; Deng, Z.; Cai, Z.; Zhang, X.; He, Z.; Cui, Z. *J. Am. Chem. Soc.* **2019**, *141*, 13454−13458.

(22) Fan, J.; Zang, Y.; Jiang, J.; Lei, J.; Xue, H. *Biosens. Bioelectron.* **2019**, *142*, 111557.

(23) Gao, X.; Wang, X.; Li, Y.; He, J.; Yu, H. *Anal. Chem.* **2018**, *90*, 8147−8153.

(24) Wu, Z.; Luo, F.; Wen, W.; Zhang, X.; Wang, S. *Anal. Chem.* **2019**, *91*, 12238−12245.

(25) Babamiri, B.; Salimi, A.; Hallaj, R. *Biosens. Bioelectron.* **2018**, *117*, 332−339.